



1 **Reviews and syntheses: Use and misuse of peak intensities from**  
2 **high resolution mass spectrometry in organic matter studies:**  
3 **opportunities for robust usage**

4

5 William Kew<sup>1</sup>, Allison Myers-Pigg<sup>2</sup>, Christine H. Chang<sup>2</sup>, Sean M. Colby<sup>2</sup>, Josie Eder<sup>1</sup>, Malak  
6 M. Tfaily<sup>3</sup>, Jeffrey Hawkes<sup>4</sup>, Rosalie K. Chu<sup>1</sup>, James C. Stegen<sup>2\*</sup>

7

8 <sup>1</sup>Environmental Molecular Sciences Laboratory, Richland, WA 99352, USA

9 <sup>2</sup>Pacific Northwest National Laboratory, Richland, WA 99352, USA

10 <sup>3</sup>Department of Environmental Science, University of Arizona, Tucson, AZ, 85719, USA

11 <sup>4</sup>Department of Chemistry, University of Uppsala, Uppsala, 75124, Sweden

12

13 \*Correspondence to: James C. Stegen ([James.Stegen@pnnl.gov](mailto:James.Stegen@pnnl.gov))

14 **Abstract**

15 Earth's biogeochemical cycles are intimately tied to the biotic and abiotic processing of organic matter (OM).  
16 Spatial and temporal variation in OM chemistry is often studied using high resolution mass spectrometry (HRMS).  
17 An increasingly common approach is to use ecological metrics (e.g., within-sample diversity) to summarize high-  
18 dimensional HRMS data, notably Fourier transform ion cyclotron resonance MS (FTICR MS). However, problems  
19 arise when HRMS peak intensity data are used in a way that is analogous to abundances in ecological analyses (e.g.,  
20 species abundance distributions). Using peak intensity data in this way requires the assumption that intensities act as  
21 direct proxies for concentrations, which is often invalid. Here we discuss theoretical expectations and provide  
22 empirical evidence why concentrations do not map to HRMS peak intensities. The theory and data show that  
23 comparisons of the same peak across samples (within-peak) may carry information regarding variation in relative  
24 concentration, but comparing different peaks (between-peak) within or between samples does not. We further  
25 developed a simulation model to study the quantitative implications of both within-peak and between-peak errors  
26 that decouple concentration from intensity. These implications are studied in terms of commonly used ecological  
27 metrics that quantify different aspects of diversity and functional trait values. We show that despite the poor  
28 linkages between concentration and intensity, the ecological metrics often perform well in terms of providing robust  
29 qualitative inferences and sometimes quantitatively-accurate estimates of diversity and trait values. We conclude  
30 with recommendations for using peak intensities in an informed and robust way for natural organic matter studies. A  
31 primary recommendation is the use and extension of the simulation model to provide objective, quantitative  
32 guidance on the degree to which conceptual and quantitative inferences can be made for a given analysis of a given  
33 dataset. Without objective guidance, researchers that use peak intensities are doing so with unknown levels of  
34 uncertainty and bias, potentially leading to spurious scientific outcomes.

35



## 36 1 Introduction

37 Organic matter (OM) plays a central role in Earth's biogeochemical cycles, and is both a resource for and product of  
38 metabolism. The detailed chemistry of OM (e.g., nominal oxidation state) can modulate and reflect biogeochemical  
39 rates and fluxes within and across ecosystems (e.g., LaRowe and Van Cappellen, 2011; Boye et al., 2017;  
40 Garayburu-Caruso et al., 2020), yet our understanding of this complexity is limited by our analytical abilities to  
41 view it (Steen et al., 2020; Hedges et al., 2000; Hawkes and Kew, 2020a). Given the importance of OM chemistry to  
42 biogeochemical cycling, there is a need to understand how and why that chemistry varies through space and time.  
43 To help meet this need, there has been growing interest in using concepts and methods from ecology to study the  
44 chemogeography and chemodiversity of OM in a variety of ecosystems (e.g., Kujawinski et al., 2009; Kellerman  
45 et al., 2014; Tanentzap et al., 2019; Danczak et al., 2021). This is a promising approach as there are many conceptual  
46 parallels between the chemical species that comprise OM and the biological species that comprise ecological  
47 communities (Danczak et al., 2020).

48  
49 The most fundamental ecological data type is the species-by-site matrix. This matrix indicates how many individuals  
50 of each species occur in each sampled community. Ecologists use species-by-site matrices to ask myriad questions  
51 related to biological diversity. Two common analyses are known as  $\alpha$ -diversity and  $\beta$ -diversity, and there are  
52 numerous metrics for each (Whittaker, 1972; Anderson et al., 2011).  $\alpha$ -diversity measures the diversity within a  
53 given community.  $\beta$ -diversity has been variously defined, but essentially measures variation in composition across  
54 communities. Both  $\alpha$ -diversity and  $\beta$ -diversity can be quantified using presence-absence data or they can include  
55 estimates of each species' relative abundance within and between communities (Fig. 1).

56  
57 The chemistry of OM is commonly studied using high resolution mass spectrometry (HRMS) techniques (e.g.,  
58 Hawkes and Kew, 2020b). Specifically, Fourier transform mass spectrometry (FTMS) techniques are predominantly  
59 used, i.e., Orbitrap or Ion Cyclotron Resonance (ICR) MS. At present, the highest resolution approach for untargeted  
60 analysis of OM is via a 21 Tesla FTICR MS (Marshall et al., 1998; Bahureksa et al., 2021). The output data  
61 produced is a spectrum containing peaks represented by a signal intensity (Fig. 2 y-axis) and a mass-to-charge ratio  
62 ( $m/z$ ) (Fig. 2 x-axis), which is equivalent to the mass for singly charged ions as routinely detected in natural organic  
63 matter (NOM) measurements. In turn, regardless of the type of MS instrument used, the MS data inherently lead to  
64 an OM peak-by-sample data matrix akin to an ecological species-by-site data matrix. The high resolution data from  
65 MS often results in a large matrix, wherein a single sample may contain thousands to tens of thousands of peaks. To  
66 take advantage of these rich data, HRMS data have been analyzed using the same  $\alpha$ -diversity and  $\beta$ -diversity metrics  
67 that are commonly used by ecologists to study biological diversity (e.g., Kellerman et al., 2014). This is exciting as  
68 it allows the same conceptual questions and quantitative frameworks to be applied to biological (e.g., microbial  
69 communities) and chemical (i.e., OM) components that directly interact with each other within ecosystems (Lucas et  
70 al., 2016; Osterholz et al., 2016; Li et al., 2018; Tanentzap et al., 2019; Danczak et al., 2020, 2021).

71  
72 The use of ecological metrics with MS data is particularly common with FTMS datasets, and contains great potential  
73 to continue leveraging concepts from ecology in high-resolution OM analyses. However, when FTMS peak intensity  
74 data are used in the estimations of  $\alpha$ -diversity,  $\beta$ -diversity, and related ecological analyses (e.g., 'species' abundance  
75 distributions), potential problems can arise. At the root of these problems lies the assumption that differences in peak  
76 intensity are proportional to differences in concentrations of the associated molecules. Consequently, the biases and  
77 uncertainties introduced by relying on this assumption are unclear. In certain situations, however, peak intensity-  
78 based ecological analyses of MS data can provide valid information—even when the underlying assumption is  
79 invalid—and the extent to which such situations exist is likewise unclear. To help advance the robust use of FTMS  
80 datasets that has been emerging in environmental science studies over the last few decades, we review the  
81 theoretical reasons why between-peak intensities do not correspond to differences in concentration, provide  
82 empirical support for our assertions, use *in silico* studies to quantify the associated impacts on ecological analyses,



83 provide practical recommendations, and propose a path forward that may eventually enable improved usage of  
84 FTMS peak intensities for quantification.

## 85 **2 Theoretical Limitations**

86 To address why peak intensities in FTMS cannot be used to infer between-peak changes in concentration, we review  
87 critical theoretical concepts about mass spectrometry. We focus on FTMS (i.e., FTICR and Orbitrap), but many of  
88 the principles and limitations—especially ionization and ion transmission—are applicable across all MS platforms.  
89 In this section, we highlight three main mass spectrometry considerations: ionization, ion transfer, and ion signal  
90 detection in the context of a generalized commercial FTICR mass spectrometer. Theoretical limitations have two  
91 main practical implications tied to within-peak and between-peak comparisons (Fig. 2). Here, we define within-peak  
92 comparison as comparing the same feature ( $m/z$  or molecular formula) across different sample spectra (i.e., within  
93 two or more sample spectra), whereas between-peak comparison occurs between different features ( $m/z$  or molecular  
94 formulas) across the same spectra.

95  
96 The first implication is that if instrument parameters are kept consistent, within-peak/between-sample biases are  
97 minimized, though between-peak/within-sample biases are inherently unavoidable. The second implication is that  
98 because of inherent sample and matrix variation and subsequent effects, between-peak/between-sample biases can  
99 be significant and may be indeterminable.

### 100 **2.1 Ionization Biases**

101 Electrospray ionization (ESI), the most commonly used technique for generating ions from NOM samples, is a ‘soft’  
102 ionization technique that predominantly yields intact molecular ions. Generally, ESI of NOM samples produces  
103 protonated or deprotonated ion types (positive or negative polarity, respectively), which can only be formed if some  
104 pre-existing basic or acidic functionality is available in the molecule to support this. ESI also commonly produces  
105 adduct ions, such as sodium adducts  $[M+Na]^+$  in positive mode and chloride adducts  $[M+Cl]^-$  in negative mode. The  
106 ionization efficiency of any given molecule depends on its structure, pKa, sample matrix and composition (Kruve et  
107 al., 2014). Ionization suppression occurs when multiple species are present in a sample, and the ionization efficiency  
108 of one analyte is altered by the presence of another (Ruddy et al., 2018). These issues all confound when dealing  
109 with complex samples with unknown compositions. While users can apply controls to account for some matrix  
110 differences (concentration, solvent, pH), the unknown (and unknowable) differences in molecular composition of  
111 complex mixtures cannot be accounted for, and therefore comparison of peak intensities in different samples is  
112 prone to uncertainty.

113  
114 Importantly, in these highly complex samples, one detected peak commonly combines signals from multiple  
115 different isomers, i.e., the same molecular formula but with a different structure. While the different structural  
116 features impact the ionization efficiency of a given molecule, the recorded spectrum shows the superposition of  
117 these isomers. To date, no liquid chromatography (Kim et al., 2019; Han et al., 2021) or ion mobility separation  
118 (Tose et al., 2018; Leyva et al., 2020) technique has demonstrated sufficient resolution for the most complex of  
119 samples (such as NOM), instead yielding broad distributions in these orthogonal dimensions. Therefore, not only  
120 must we apply extreme caution in inferring chemical properties from molecular formula alone, but we must also be  
121 aware of underlying subtleties that may distort comparisons of molecular formula and peak intensities within  
122 samples such as the presence of isomers.

### 123 **2.2 Ion transmission**

124 Before ions can be detected in the (ion) trap, they must be transmitted from the instrument source to the trap. Ion  
125 transmission, including ion accumulation, is not unbiased. Ions are manipulated through the instrument ion optics,  
126 across differential pressure regimes, using radiofrequency (RF) and direct current (DC) potentials to guide, focus,



127 and accumulate the ions. The specific values of these parameters have effects on the mass ranges transmitted.  
128 Further, the specific timings, geometries, and vacuum regimes all have effects upon ion transmission efficiency and  
129 biases. For this reason, quantitative comparison of intensities across widely differing  $m/z$  is not directly possible.  
130  
131 In FTMS, packets of ions are accumulated and ‘cooled’ in a trap prior to their transmission to the analyzer cell (Fig.  
132 3 Panel A section d; Senko et al., 1997; Makarov et al., 2006). The duration of time in which ions are accumulated is  
133 varied to yield an optimal ion population for the analyzer cell, which has a finite charge capacity. The duration of  
134 this event has been directly observed to change the relative ion populations (Cao et al., 2016). Thus, when balancing  
135 the need for controlled ion populations - critical for a high resolution, high fidelity measurement - and minimal  
136 variation in ion accumulation time, there is a risk of further biasing the relative ion intensities.  
137  
138 Finally, time-of-flight biases come into play in FTICR MS. Ions are transmitted from the ion accumulation trap to  
139 the ICR cell along one or more transfer multipoles (Fig. 3 Panel A section e). The distance between ion  
140 accumulation trap and ICR cell may be quite long, e.g., 2.4 meters on a 21 Tesla instrument (Shaw et al., 2016), and  
141 therefore the time required for ions to travel this distance (the ‘time-of-flight’, a millisecond or longer) may cause  
142 dispersion in the ion packet (Fig. 3 Panel B). While the packet of ions may leave the accumulation trap  
143 simultaneously, because smaller ions travel faster the packet arrives at the analyzer cell as a dispersed distribution of  
144 ions. Therefore, only a subset of this population, with regards  $m/z$ -range and ion energies, is optimally trapped in the  
145 ICR cell. Thus, these biases in ion transmission do not allow for quantitative comparison of peak intensities between  
146 ions with differing  $m/z$  ratios.

### 147 **2.3 Ion signal detection**

148 To directly use FTMS peak intensities quantitatively, we must first understand how those intensities arise and the  
149 biases which can affect them. In ion trapping measurements, such as FTICR and Orbitrap MS, the motion of ions  
150 within a static magnetic (ICR) or electric (Orbitrap) field induces an image current upon detection electrodes. The  
151 frequency of this motion is proportional to the mass-to-charge ratio ( $m/z$ ) of the ion, while the intensity of the signal  
152 is proportional to the abundance of the ion in the trap, the proximity of the ion to the electrode (Kaiser et al., 2013),  
153 and the charge state of the ion (Wörner et al., 2020). Thus, at a first approximation, the signal intensity between  
154 different  $m/z$  ions could be compared provided they are excited to the same radius (ICR) and have the same charge  
155 state (Fig. 3 Panels B, C). However, these provisions are not always met. Ions with very close frequencies, which are  
156 not fully resolved, may affect each other’s signal intensity, and the Fourier transform does not allow for extremely  
157 accurate relative quantification of ion abundance between peaks (Makarov et al., 2019). With FTICR, most  
158 commercial (e.g., Bruker) instruments use a CHIRP, or frequency-swept, excitation pulse which does not excite all  
159 ions to exactly the same radii (Kaiser et al., 2013). In addition, while most ions in NOM mass spectra are singly  
160 charged, some mass spectra contain multiply charged interferences (Smith et al., 2018; Patriarca and Hawkes, 2021).  
161 Still, in both instrument types, signal intensities may be used to describe the ion populations quantitatively provided  
162 that the charge states are the same, a flat-excitation profile is used (or the ions are sufficiently close in frequency  
163 space such that they are excited to the same radii), and the user clearly understands that the ion population in the trap  
164 may not accurately reflect the molecular composition of the sample.

165  
166 Within a well-designed experiment and a constrained sample set, many of these points may be mitigated. However,  
167 objectively proving the degree of mitigation is non-trivial, and there remains great uncertainty about the relationship  
168 between peak intensity and molecular concentrations, particularly for complex matrices such as NOM. Furthermore,  
169 as shown in a recent interlaboratory study (Hawkes et al., 2020), measuring the same samples with different  
170 instrumentation can lead to differing results, thus further highlighting potential pitfalls in quantitative analysis of  
171 these data.



## 172 **3 Empirical Limitations**

173 Despite the aforementioned fundamental and theoretical limitations and uncertainties in using peak intensity data, it  
174 is still helpful to demonstrate these limitations with real-world empirical measurements. In this section, we  
175 demonstrate, with ideal and non-ideal samples, the non-quantitative nature of these measurements.

### 176 **3.1 Direct comparison of signal intensities in idealized samples is problematic**

177 In the ideal case, samples are analyzed with identical matrices, equivalent concentrations for each compound, and  
178 free from competitive ionization/ionization suppression (Ruddy et al., 2018). However, even in this ideal case,  
179 different molecules ionize with different efficiencies, and thus their signal intensities are not equal. To demonstrate  
180 the non-equal response for various analytes in various conditions, we acquired a series of contemporaneous mass  
181 spectra of several compounds in different conditions. First, in Fig 4A, we prepared three dilution ladders of three  
182 pure compounds - analyzed separately - in pure methanol. Clearly, these three molecules yield starkly different  
183 signal intensities for otherwise identical conditions, and thus directly comparing their intensities would not be a  
184 valid means to infer their relative concentrations in solution. At an extreme, trehalose, a carbohydrate, yields nearly  
185 as little signal at 500ppb as sinapic acid does at 200ppb. Even between the two structures containing a carboxylic  
186 acid moiety - a typical indicator of good negative mode ESI response - there is a significant difference in signal  
187 intensity. Thus, directly comparing the signal intensities of different ions - even in idealized situations - cannot be  
188 used as a proxy for concentration or abundance determination absent a calibration curve.

189  
190 Subsequently, we highlight the challenge of comparing ions of the same exact mass. Here, in Fig 4B, we again  
191 prepared dilution ladders of three pure compounds in methanol, however these are all structural isomers with the  
192 same molecular formula and thus exact mass. Again, a stark difference in signal intensity is observed, even between  
193 nominally similar structures. This issue is particularly troubling for direct infusion measurements of complex  
194 mixtures, where we do not, and cannot, know the structural identity of individual peaks, and instead are limited to  
195 molecular formulas. Thus, if we compare peaks with the same exact mass, same molecular formula, between  
196 different samples, we cannot be sure that they are the same molecule, and thus again comparing their signal  
197 intensities as a proxy for abundance is problematic. Additionally, structural isomers can have vastly different  
198 ecological/biogeochemical function, and therefore this consideration is important to note for subsequent  
199 interpretations of NOM samples. Further complicating this issue is the known fact that in highly complex mixtures  
200 like organic matter, most - or all - peaks are actually the superposition of multiple different isomeric compounds.  
201 Demonstrated by chromatography (Kim et al., 2019) or ion mobility separations (Leyva et al., 2019), or by statistical  
202 inference of tandem mass spectrometry (Zark et al., 2017), each peak may be several isomers of various relative  
203 intensities. Thus, even if the same isomers were present across samples, it cannot be known that their relative  
204 abundances are the same - and again, it is problematic to directly compare the intensities of signal corresponding to  
205 nominally the same molecular formula across different mass spectra.

206  
207 One caveat with the above experiments, of course, is that it is a direct infusion measurement. The chemicals used  
208 were nominally pure, but any trace impurity - either from their production and isolation, or from sample preparation  
209 - may impact the measured signal intensity. Which leads us to the next point - matrix effects are intrinsically  
210 challenging to control for, and have significant impacts on mass spectra.

### 211 **3.2 Matrix effects substantially impact signal intensities in complex mixtures**

212 Of course, analyses are often performed on complex mixtures, containing a diverse range of thousands of molecules  
213 of unknown structures and relative concentrations. Furthermore, samples often contain 'inorganic' interferences,  
214 such as salts. Routinely, scientists will desalt samples with solid phase extraction, but such processes can leach  
215 impurities into the sample, don't necessarily remove all interferences, and can remove select pools of NOM due to  
216 their functionalities, depending on the sorbent or resin (Raeke et al., 2016; Li et al., 2017). As such, real world non-



217 ideal samples contain a multitude of matrix effects and sources for ionization suppression, or adduct formation,  
218 which yield spectra that are even more challenging to quantitatively interpret.

219

220 To explore the impacts of matrix effects (Fig. 4C-E), we prepared solutions of six different pure compounds at a  
221 fixed concentration (100ppb) in three different solvent systems - pure methanol, methanol from elution off of a  
222 BondElut SPE cartridge, and methanol from elution off of a BondElut SPE cartridge which had been loaded with  
223 artificial river water (ARW). Additionally, we added a complex mixture - Suwannee River Fulvic Acid (SRFA), at  
224 six different concentrations, to each sample. Again, samples were analyzed independently but contemporaneously  
225 on the same instrument to mirror a real study.

226

227 In methanol only solvent, with no addition of SRFA, the six compounds - as expected - yield different signal  
228 intensities (Fig. 4C), further confirming what was previously observed. As the concentration of SRFA is increased to  
229 2 ppm, the relative signal intensity increases for some of these analytes - possibly as a function of endogenous  
230 molecules with the same molecular formula as those spiked in - but decreases for others. Above 2 ppm of SRFA,  
231 however, all signals for our reference compounds are substantially decreased, most likely as a result of competitive  
232 ionization effects of the addition of the complex mixture.

233

234 Use of an 'impure' methanol solvent, i.e., the eluent from a SPE blank (Fig. 4D) or from an SPE of artificial river  
235 water (Fig. 4E), results in even more ionization suppression and differential signal response. In both cases, the  
236 maximum signal intensity is only 20% of what was seen in pure methanol (Fig. 4C), indicating that the leachate or  
237 residual salts from the SPE protocol impacted sensitivity. Further, here only two analytes (aesculin and chlorogenic  
238 acid) ionize well at all, with the other 4 yielding poor or no signal. Addition of SRFA, again, decreases signal  
239 intensity, though at 40 ppm SRFA some minor features increase, likely due to endogenous features with the same  
240 molecular formula as our standards.

241

242 Cumulatively, empirical evidence and instrumental theory demonstrate that it is not possible - with direct infusion  
243 measurements of complex mixtures - to directly compare signal intensities as a proxy for molecular abundance  
244 between different peaks within a spectrum, or between the same peak across spectra, even in idealized cases.  
245 Strategies to use calibration curves will fail due to unknown structural composition, and established normalization  
246 techniques cannot factor in the large range of sources of experimental variation. That said, there may be cases where  
247 a high-level comparison of trends can yield valid semi-quantitative comparisons between spectra, relying on a  
248 statistical aggregation of individually unreliable trends. Additionally, modeling of constrained systems may allow  
249 for improved, data-driven and mechanistic based machine-learning data normalization strategies.

250

#### 251 **4 Conceptual implications for use of ecological metrics**

252

253 The preceding sections have shown both theoretically and empirically that there are challenges to using HRMS peak  
254 intensities as proxies for relative changes in concentrations of organic molecules. The implication is that there may  
255 be specific kinds of ecologically-inspired analyses (e.g., Fig. 1) that are or are not appropriate to use with HRMS  
256 peak intensity data. To understand what may or may not be a valid analysis, it is critical to differentiate analyses into  
257 two classes: those based on within-peak intensity comparisons and those based on between-peak intensity  
258 comparisons (Fig. 2). As noted above, within-peak is based on comparing the same feature ( $m/z$  or molecular  
259 formula) across spectra/samples, whereas between-peak compares different features ( $m/z$  or molecular formulas)  
260 across and within spectra/samples.

261

262 Analyses using between-peak intensity comparisons are the most likely to be problematic. To help clarify why this  
263 is, consider an ecological setting in which a researcher aims to quantify  $\alpha$ -diversity and  $\beta$ -diversity (Fig. 1) of tree  
264 communities (Fig. 5, left-side). The researcher will likely set up a plot of a given size and then directly count the





265 number of each tree species in each plot. This generates the species-by-site matrix filled with directly observed  
266 abundance counts for each species. In such a situation, the ability of the researcher to observe individuals of each  
267 species does not vary appreciably across species because each tree is not moving and our ability to see it is not  
268 influenced by environmental factors. In turn, the number of individuals observed for a given species is quantitatively  
269 comparable to the number of individuals observed for all other species in the plot. The assumption that differences  
270 in observed abundances carry robust information about differences in actual abundances is thus supported. In turn, it  
271 is valid to use relative abundances to compute  $\alpha$ -diversity such as via Shannon evenness (Elliott et al., 1997;  
272 Mouillot and Leprêtre, 1999; Redowan, 2015). Furthermore, the ability to observe each species is the same across  
273 communities. In turn, it is valid to use relative abundances to compute  $\beta$ -diversity (e.g., via Bray-Curtis; Anderson et  
274 al., 2011) or conduct any other ecological analysis that uses abundance data (e.g., species abundance distributions  
275 McGill et al., 2007).

276  
277

278 We contrast this tree community example with another ecological setting. Consider a researcher studying bird  
279 communities (Fig. 5, right side) that estimated species abundances solely based on the number of times an observer  
280 hears the call of a given species. In this case, those species that call more frequently and/or more loudly (more likely  
281 to be heard), will be inferred to have higher abundance even if all species in the community have the same  
282 abundance. That is, such a method generates data that may indicate which species are present, but the ‘call counts’  
283 do not carry reliable information regarding absolute or between-species relative abundances. Follow-on analyses of  
284  $\alpha$ -diversity and  $\beta$ -diversity should, therefore, be limited to approaches that use presence/absence data, and species  
285 abundance distributions cannot be quantified.

286

287 If we continue with the bird community example and assume that the detectability of a given bird species is  
288 consistent across sampled locations (or times), then it would be appropriate to examine variation in within-species  
289 call counts. This within-species analysis is directly analogous to the HRMS within-peak time series analysis in  
290 Merder et al. (2021), discussed below. However, if call counts of a given species are suppressed by the  
291 presence/abundance of other species, then call counts of a given species do not indicate an increase in its abundance.  
292 This is directly analogous to influences of the OM matrix: if the presence/abundance of a given organic molecule  
293 modifies the ionization of other molecules, then within-peak changes in intensity do not indicate changes in their  
294 concentrations. In turn, analyses based on within-peak intensity comparisons are not always valid, especially if there  
295 are significant cross-sample changes in the OM matrix.

296

297 Unfortunately, as demonstrated in the previous sections, HRMS data align with the bird community examples and  
298 never reflect the tree community example. The unique chemistry of every molecule fundamentally results in  
299 different ionization properties for other molecules. Thus, the differing physics of each molecule strongly influences  
300 between-peak differences in peak intensity. Those molecules that ionize more easily result in higher peak intensities,  
301 which is akin to bird species that call more frequently or more loudly resulting in a larger number of ‘call counts.’ In  
302 turn, between-peak differences in intensity cannot be used as a proxy to indicate between-peak differences in  
303 concentration. This could invalidate the application of ecological metrics that use between-peak differences in  
304 intensity.

305

306 In contrast to between-peak comparisons, within-peak comparisons examine changes in relative intensity of a single  
307 peak across samples. Such within-peak comparisons may be repeated independently for each peak of interest in a  
308 given dataset. For example, Merder et al. (2021) quantified temporal dynamics of individual HRMS peaks and then  
309 binned peaks into different groups with characteristic temporal fluctuations. In those analyses, peak intensities were  
310 not compared between peaks. Instead, the temporal dynamics of each peak was compared to temporal dynamics of  
311 other peaks. The underlying assumption of this type of analysis is that a between-sample increase in the intensity of  
312 a given peak can be used as a robust proxy of a between-sample increase in concentration of that peak. Materials  
313 presented in the previous sections indicate that this assumption can be met in some instances when using HRMS



314 data. However, great care is required with strong attention paid to assumptions of analysis methods. For example,  
315 using Pearson correlation makes the assumption that concentration of a given peak is a *linear* function of changes in  
316 its peak intensity. We showed above (Fig. 4) that assumption is not always valid even in ideal conditions. Using a  
317 Spearman correlation avoids this assumption because it is based on ranks. That is, using Spearman (e.g., Kellerman  
318 et al., 2014) makes the more realistic assumption (for FTICR MS data) that an increase in concentration of a given  
319 peak is reflected as an increase in its peak intensity, without assuming any statistical or mathematical form of that  
320 relationship.

321

## 322 **5 Quantitative impacts**

323

324 The previous sections show that between-peak changes in peak intensity do not accurately reflect between-peak  
325 changes in abundance (Fig. 4). This violates a fundamental assumption of abundance-based ecological analyses:  
326 proxies of abundance (e.g., peak intensity) must reflect actual abundance. In turn, it is tempting to infer that mass  
327 spectrometry peak intensities cannot be used at all in ecological analyses. However, the impacts of violating the  
328 assumption have not been directly quantified. This is a significant gap considering the growing number of  
329 publications that use peak intensities to compute abundance-based ecological metrics over the last couple decades.

330

331 Therefore, there is a need to quantitatively understand biases and uncertainties introduced in ecological metrics  
332 (e.g.,  $\alpha$  and  $\beta$  diversities) and/or models when peak intensity does not reflect abundance or concentration. To  
333 provide an initial evaluation, we developed an *in silico* simulation model that generates synthetic data, introduces  
334 specific kinds of error commonly found with HRMS datasets (discussed above in detail), and computes within-  
335 sample (e.g., Shannon diversity) and between-sample (e.g., Bray-Curtis) ecological metrics (Fig. 6). This allows for  
336 comparison between true values of the metrics and the values observed after each type of error is introduced, which  
337 is impossible to do with non-simulated datasets. To generate synthetic data, we randomly assigned abundances to  
338 either 100 or 1000 peaks. Abundances were sampled with replacement from a Gaussian distribution that varied in  
339 mean and standard deviation across synthetic samples and across simulation iterations. Abundances were drawn  
340 twice to generate two independent samples per simulation, and the simulation was run 100 times for each number-  
341 of-peaks (100 or 1000 peaks per sample; referred to below as ‘peak richness’). The reason for variation in the  
342 Gaussian distributions was to generate synthetic samples that varied in composition within and across simulations to  
343 ensure that the ecological metrics (see below) would vary across simulations. This was necessary to evaluate how  
344 biases in the metrics varied across a broad range of metric values.

345

346 We simulated two types of error, and both can be representative of variation in ionization efficiency. The goal was  
347 to generate synthetic data that mimicked our empirical and theoretical observations in the sense that observed peak  
348 intensities did not reflect true abundances. For each type of error and within each iteration of the simulation, the  
349 error was introduced 100 times (i.e., 100 error iterations were nested within each sample-generation iteration). The  
350 first type of error was designed to diminish the between-peak relationship between observed intensity and true  
351 abundance. For this we multiplied the true abundance of each peak by a random number drawn from a uniform  
352 distribution ranging from 0 to 100. For each peak we multiplied the same random error to its abundance in each of  
353 the two synthetic samples within each iteration. The error-modified abundance of each peak in each synthetic  
354 sample was considered to be the observed peak intensity.

355

356 As expected, introducing error resulted in a relatively weak relationship between observed intensity and true  
357 abundance, with the amount of error increasing with true abundance (Fig. S1) and a median  $R^2$  of  $\sim 0.5$  (see black  
358 line in Figure 7). Between-peak differences in observed intensity were also weakly related to between-peak  
359 differences in true abundance (Fig. 8A), with a median  $R^2$  of  $\sim 0.5$  (see blue line in Figure 7). Because the same  
360 peak-level error-factor was used across both synthetic samples within a given simulation iteration, the within-peak





361 between-sample differences in observed intensity were relatively strongly correlated to within-peak between-sample  
362 differences in true abundance (Fig. 8B), with a median  $R^2$  of  $\sim 0.75$  (see the gray line in Figure 7).

363

364 The second type of error introduced represents situations in which there is variation in ionization efficiency across  
365 molecules – as in the first type of error – but that ionization efficiency also varies across samples. Molecules may  
366 vary in their ionization efficiency across samples due to changes in the composition of organic molecules and/or  
367 changes in inorganic solutes. In this case, ionization efficiency of any given molecule is due to interactions with  
368 other organic and inorganic molecules within a given sample. For this, we multiplied the true abundance of each  
369 peak by a random number drawn from a uniform distribution ranging from 0 to 100. For each iteration of the  
370 simulation this was done independently for both synthetic samples. In this way, ionization efficiency for a given  
371 peak in a given synthetic sample was independent of its ionization efficiency in the other synthetic sample. In turn,  
372 the error-modified abundance of each peak in each synthetic sample was considered to be the observed peak  
373 intensity.

374

375 We observed a relatively large influence of allowing ionization efficiency to vary randomly across samples. That is,  
376 the within-peak between-sample differences in observed intensity were relatively weakly correlated to within-peak  
377 between-sample differences in true abundance (Fig. 8B), with a median  $R^2$  of  $\sim 0.5$  (see the red line in Figure 7).  
378 Comparing this to the same relationship that emerged under the first type of error shows a much weaker relationship  
379 when ionization efficiency varies between samples (compare the gray and red lines in Figure 7). This is expected as  
380 variation in ionization efficiency will add random noise to the within-peak between-sample differences in observed  
381 peak intensity. We note that variation in ionization efficiency is independent between peaks for both the first and  
382 second types of error. The between-peak relationship summarized in Figure 7 (blue line) is, therefore, equivalent for  
383 both types of error, which is also shown by the strong similarity between Figure 8A and 8C.

384

385 To examine influences of both types of error on ecological metrics we used the initial true abundances and the error-  
386 modified abundances (i.e., observed intensity values) to calculate true and ‘observed’ values of within-sample  
387 Shannon diversity and between-sample Bray-Curtis. We also assigned a trait value to each peak and calculated true  
388 and observed sample-level mean trait values; the mean values for each sample were weighted by true abundance  
389 (true mean) or observed intensity (observed mean). To evaluate biases and uncertainty introduced by both types of  
390 error we regressed observed values for each metric against their true values. This was done independently for each  
391 level of peak richness to evaluate how bias and uncertainty vary with the number of peaks contained within a  
392 sample.

393

394 Relating ‘observed’ values of each metric to their true values revealed that the patterns observed in peak-intensity-  
395 based ecological metrics are likely to be qualitatively robust, even though quantitative biases do exist (Figs. 9-11).  
396 All three ecological metrics showed monotonic relationships between observed and true values. Uncertainty was  
397 lower when samples had 1000 peaks, relative to samples with 100 peaks; in Figures 9-11 all A/B and C/D panels  
398 have 100 and 1000 peaks, respectively. Monotonic relationships and lower uncertainty with more peaks were found  
399 for both within-sample and between-sample error; in Figures 9-11 all A/C and B/D panels have within-sample and  
400 between-sample errors, respectively. For Shannon diversity, observed values were consistently lower than true  
401 values, but all observed vs. true relationships were linear (Fig. 9). For Bray-Curtis, inclusion of between-sample  
402 error resulted in an overestimation of values and non-linear (but monotonic) relationships between observed and true  
403 values (Fig. 10). For mean trait values, the observed values had uncertainty but there were no systematic quantitative  
404 biases and the relationships between observed and true values were consistently linear (Fig. 11). Furthermore, the  
405 variation in observed values explained by true values (via a linear model) increases rapidly with the number of  
406 peaks, and sharply asymptotes beyond  $\sim 500$ -1000 peaks per sample (Fig. S2). We caution that the number of peaks  
407 needed to reach the asymptote, thereby minimizing error, is likely dataset dependent and 500-1000 peaks should not  
408 be taken as a general rule.



## 409 **6 Conclusions and Recommendations**

410 There is increasing interest in using ecological metrics to study organic matter chemistry across a broad range of  
411 environments and settings. It is vital that this growing body of work be based on rigorous use of the data to develop  
412 trust in the associated conceptual and mechanistic inferences. To do so requires deep understanding of the metrics  
413 themselves, full awareness of the limitations of the OM data from mass spectrometers, and careful use of the metrics  
414 informed by the data limitations. We suggest that studies/publications that use peak intensities need to include  
415 material that directly discusses the data limitations, what peak intensities do and do not represent (e.g., tree-like vs.  
416 bird-like data; Fig. 5), and how knowledge of those limitations was used to select specific metrics.

417  
418 We have provided both strong theoretical reasoning and empirical observations showing that peak intensities do not  
419 directly map to concentrations of the associated organic molecules within complex mixtures of organic molecules.  
420 This is particularly true for between-peak comparisons of intensity, and statistical post-hoc normalizations of peak  
421 intensity data do not solve this problem. That is, there are no situations that we are aware of in which between-peak  
422 differences in intensity indicate between-peak differences in concentration. We therefore assert that between-peak  
423 differences in intensity within HRMS data cannot be used to make direct inferences related to between-peak  
424 variation in abundance or concentration. This means that HRMS data are unlikely to provide informative ecological  
425 analyses based directly on variation in species abundances. In particular, estimation of ‘species abundance  
426 distributions’ is likely to be invalid. Analyses that bin peaks into high and low abundance groups based on between-  
427 peak differences in concentration are, likewise, almost certainly invalid. We did not directly evaluate these types of  
428 analyses, however, and we suggest that future work should expand upon the ecological metrics examined here via  
429 simulation.

430  
431 While certain ecological analyses of HRMS data are likely to be invalid, we found good performance of some  
432 common metrics. These metrics were originally designed to use relative abundances of biological species. Our  
433 simulation modeling indicated that at least some  $\alpha$ -diversity,  $\beta$ -diversity, and functional trait metrics are likely to  
434 provide valid qualitative patterns. That is, conceptual and mechanistic inferences are likely to be valid when based  
435 on analyses such as comparing peak-intensity-based ecological metrics across experimental treatments or variation  
436 along environmental gradients. The performance of intensity-weighted mean trait values was particularly good in  
437 terms of both qualitative and quantitative aspects. We emphasize that we studied a small set of metrics (Shannon  
438 diversity, Bray-Curtis, and intensity-weighted trait values) and our inferences only extend to these metrics.  
439 Fortunately, it is relatively straightforward to extend the simulation model to additional metrics (e.g., Hill numbers;  
440 Hill, 1973) and analyses (e.g., species abundance distributions; McGill et al., 2007) and we suggest that users of  
441 such datasets wanting to use additional ecological metrics/analyses test them using simulation models before  
442 applying to real-world datasets to ascertain if these metrics hold given the known biases in these analyses and  
443 metrics.

444  
445 To enable robust use of HRMS peak intensity data in future studies, we recommend use of and further development  
446 of the simulation model developed here. The simulation model is the only tool we are aware of that can provide  
447 objective guidance on what analyses are not valid and the level of uncertainty associated with valid analyses. It  
448 should not be taken as a static or mature tool, however. The model should be expanded in a number of ways by  
449 including additional ecological metrics/analyses, more than two-sample situations, other ways of modeling error,  
450 and measured levels of error between concentrations and peak intensities. This will allow each study to customize  
451 the model for their specific application. It should be possible to include the number of samples, the number of peaks  
452 in each sample, the peak intensity distributions, number of replicates, and the specific ecological analyses that will  
453 be applied. In turn, simulation model outcomes can provide objective guidance tailored to each study. One may  
454 think of the resulting guidance as akin to a power analysis whereby the simulation can indicate what can and cannot  
455 be inferred from a given dataset. For example, the model indicates that observed Bray-Curtis values have little to no  
456 correspondence to true values when Bray-Curtis is below  $\sim 0.2$  (Fig. 10B, D). Bray-Curtis near and below  $\sim 0.2$  are



457 commonly observed in HRMS studies (e.g., Hawkes et al., 2016; Derrien et al., 2018; Bao et al., 2018), and this  
458 disconnect between observations and truth is maintained even with 1000 peaks per sample (Fig. 10D). In turn,  
459 HRMS studies that observe Bray-Curtis below  $\sim 0.2$  may not be able to use those observations to make valid  
460 conceptual inferences. However, quantitative guidance must be developed for each study and we recommend that a  
461 version of the simulation model should be used by all future studies using peak intensities to conduct ecological  
462 analyses of HRMS data. It may be that in time we understand the general rules well enough to leave the simulation  
463 behind, but for now, failing to use it (or a similar tool) leaves analyses open to criticism and potentially spurious  
464 inferences.

465  
466 In addition to further use and development of the simulation model, we recommend translation of other modeling  
467 approaches for use with HRMS data. Two potential approaches are based in machine learning and hierarchical  
468 modeling. Machine learning could be used within very tightly controlled systems to understand the magnitude and  
469 nature of non-quantitative biases that disconnect peak intensity from concentration. In this case, one could model the  
470 instrument response for a diverse chemical space in typical environmental samples to learn how measured signal  
471 intensities may relate to starting concentrations. Even if such a model does not yield high-accuracy results, it may  
472 nonetheless help understand error, biases, and robust use of peak intensity data. Furthermore, such a model would be  
473 constrained to the system it was built around, and application outwith this system could be wrong. Potentially in  
474 concert with machine learning, hierarchical modeling could be translated from its application in ecological analyses  
475 (Iknayan et al., 2014) for use with HRMS. This approach has been used to model sources of error that lead to  
476 variation in detectability across biological species, such as variation in species visibility (e.g., Dorazio and Royle,  
477 2005). In turn, data can essentially be corrected by accounting for the modeled sources of error (Roth et al., 2018),  
478 even revealing ‘hidden diversity’ (Richter et al., 2021). Machine learning could be used to understand sources of  
479 error and, in turn, inform hierarchical models aimed at improving the mapping between peak intensity and  
480 concentration. If successful, this would increase the quality of information provided by peak intensities in both  
481 existing and future datasets, thereby enabling more robust conceptual and mechanistic inferences.

482  
483 In summary, HRMS has many strengths and weaknesses just like any analytical platform. Careful use of peak  
484 intensity data informed by objective, model-based guidance can overcome some of its weaknesses. Despite peak  
485 intensities not reflecting concentrations, ecological metrics overall appear to perform well. This is likely due to the  
486 law of large numbers as HRMS, especially FTICR MS, datasets often contain 1000 or more peaks per sample. Our  
487 simulation results indicate that large numbers of identified peaks allow ecological metrics to essentially track  
488 towards their true value. We are encouraged by this outcome and look forward to further applications of ecological  
489 metrics, concepts, and theory to organic matter chemistry.

## 490 491 **7 Code Availability**

492  
493 R code for running the simulation models is available on GitHub: [https://github.com/stegen/Peak\\_Intensity\\_Sims](https://github.com/stegen/Peak_Intensity_Sims).  
494 Python code used to process the empirical data and to generate the associated figures will be available upon  
495 publication.

## 496 497 **8 Data Availability**

498  
499 Raw and processed data will be made publicly available upon manuscript acceptance.  
500

## 501 502 **9 Author Contributions**

503 WK contributed to conceptualization, experimental data curation, formal analysis, methodology, software,  
504 visualization, writing-original draft, writing-review/editing; AMP contributed to conceptualization, methodology,



505 visualization, writing-original draft, writing-review/editing; CHC and SMC contributed to investigation and writing-  
506 review/editing; JE contributed to sample preparation and writing-review/editing; MMT contributed to  
507 conceptualization, methodology, writing-review/editing; JH contributed to conceptualization and writing-  
508 review/editing; RKC contributed to project administration, conceptualization, experimental data curation,  
509 methodology, writing-review/editing; JCS contributed to conceptualization, simulation data curation, formal  
510 analysis, funding acquisition, investigation, methodology, software, visualization, writing-original draft, writing-  
511 review/editing.

## 512 **10 Competing interests**

514

515 The authors declare that they have no conflict of interest.

516

## 517 **11 Acknowledgements**

518

519 A portion of this research was performed on a project award (doi:10.46936/intm.proj.2020.51667/60000248) from  
520 the Environmental Molecular Sciences Laboratory, a DOE Office of Science User Facility sponsored by the  
521 Biological and Environmental Research program under Contract No. DE-AC05-76RL01830. JCS was also  
522 supported by an Early Career Award (grant 74193) to JCS at Pacific Northwest National Laboratory (PNNL), a  
523 multiprogram national laboratory operated by Battelle for the United States Department of Energy under contract  
524 DE-AC05-76RL01830. We thank Alan Roebuck for useful feedback on the manuscript, Nathan Johnson for  
525 graphics development, Charles T. Resch for supplying the artificial river water, Patricia Miller and Jason Toyoda for  
526 lab support.

## 527 **12 References**

- 528 Anderson, M. J., Crist, T. O., Chase, J. M., Vellend, M., Inouye, B. D., Freestone, A. L., Sanders, N. J., Cornell, H.  
529 V., Comita, L. S., Davies, K. F., Harrison, S. P., Kraft, N. J. B., Stegen, J. C., and Swenson, N. G.: Navigating  
530 the multiple meanings of  $\beta$  diversity: a roadmap for the practicing ecologist, *Ecol. Lett.*, 14, 19–28,  
531 <https://doi.org/10.1111/j.1461-0248.2010.01552.x>, 2011.
- 532 Bahureksa, W., Tfaily, M. M., Boiteau, R. M., Young, R. B., Logan, M. N., McKenna, A. M., and Borch, T.: Soil  
533 Organic Matter Characterization by Fourier Transform Ion Cyclotron Resonance Mass Spectrometry (FTICR  
534 MS): A Critical Review of Sample Preparation, Analysis, and Data Interpretation, *Environ. Sci. Technol.*, 55,  
535 9637–9656, <https://doi.org/10.1021/acs.est.1c01135>, 2021.
- 536 Bao, H., Niggemann, J., Luo, L., Dittmar, T., and Kao, S.-J.: Molecular composition and origin of water-soluble  
537 organic matter in marine aerosols in the Pacific off China, *Atmos. Environ.*, 191, 27–35,  
538 <https://doi.org/10.1016/j.atmosenv.2018.07.059>, 2018.
- 539 Boye, K., Noël, V., Tfaily, M. M., Bone, S. E., Williams, K. H., Bargar, J. R., and Fendorf, S.: Thermodynamically  
540 controlled preservation of organic carbon in floodplains, *Nat. Geosci.*, 10, 415–419,  
541 <https://doi.org/10.1038/ngeo2940>, 2017.
- 542 Cao, D., Lv, J., Geng, F., Rao, Z., Niu, H., Shi, Y., Cai, Y., and Kang, Y.: Ion Accumulation Time Dependent  
543 Molecular Characterization of Natural Organic Matter Using Electrospray Ionization-Fourier Transform Ion  
544 Cyclotron Resonance Mass Spectrometry, *Anal. Chem.*, 88, 12210–12218,  
545 <https://doi.org/10.1021/acs.analchem.6b03198>, 2016.
- 546 Danczak, R. E., Chu, R. K., Fansler, S. J., Goldman, A. E., Graham, E. B., Tfaily, M. M., Toyoda, J., and Stegen, J.  
547 C.: Using metacommunity ecology to understand environmental metabolomes, *Nat. Commun.*, 11, 6369,  
548 <https://doi.org/10.1038/s41467-020-19989-y>, 2020.
- 549 Danczak, R. E., Goldman, A. E., Chu, R. K., Toyoda, J. G., Garayburu-Caruso, V. A., Tolić, N., Graham, E. B.,  
550 Morad, J. W., Renteria, L., Wells, J. R., Herzog, S. P., Ward, A. S., and Stegen, J. C.: Ecological theory



- 551 applied to environmental metabolomes reveals compositional divergence despite conserved molecular  
552 properties, *Sci. Total Environ.*, 788, 147409, <https://doi.org/10.1016/j.scitotenv.2021.147409>, 2021.
- 553 Derrien, M., Lee, Y. K., Shin, K.-H., and Hur, J.: Comparing discrimination capabilities of fluorescence  
554 spectroscopy versus FT-ICR-MS for sources and hydrophobicity of sediment organic matter, *Environ. Sci.*  
555 *Pollut. Res.*, 25, 1892–1902, <https://doi.org/10.1007/s11356-017-0531-z>, 2018.
- 556 Dorazio, R. M. and Royle, J. A.: Estimating Size and Composition of Biological Communities by Modeling the  
557 Occurrence of Species, *J. Am. Stat. Assoc.*, 100, 389–398, <https://doi.org/10.1198/016214505000000015>,  
558 2005.
- 559 Elliott, K. J., Boring, L. R., Swank, W. T., and Haines, B. R.: Successional changes in plant species diversity and  
560 composition after clearcutting a Southern Appalachian watershed, *For. Ecol. Manag.*, 92, 67–85,  
561 [https://doi.org/10.1016/S0378-1127\(96\)03947-3](https://doi.org/10.1016/S0378-1127(96)03947-3), 1997.
- 562 Garayburu-Caruso, V. A., Stegen, J. C., Song, H.-S., Renteria, L., Wells, J., Garcia, W., Resch, C. T., Goldman, A.  
563 E., Chu, R. K., Toyoda, J., and Graham, E. B.: Carbon Limitation Leads to Thermodynamic Regulation of  
564 Aerobic Metabolism, *Environ. Sci. Technol. Lett.*, 7, 517–524, <https://doi.org/10.1021/acs.estlett.0c00258>,  
565 2020.
- 566 Han, L., Kaesler, J., Peng, C., Reemtsma, T., and Lechtenfeld, O. J.: Online Counter Gradient LC-FT-ICR-MS  
567 Enables Detection of Highly Polar Natural Organic Matter Fractions, *Anal. Chem.*, 93, 1740–1748,  
568 <https://doi.org/10.1021/acs.analchem.0c04426>, 2021.
- 569 Hawkes, J. A. and Kew, W.: 4 - High-resolution mass spectrometry strategies for the investigation of dissolved  
570 organic matter, in: *Multidimensional Analytical Techniques in Environmental Research*, edited by: Duarte, R.  
571 M. B. O. and Duarte, A. C., Elsevier, 71–104, <https://doi.org/10.1016/B978-0-12-818896-5.00004-1>, 2020a.
- 572 Hawkes, J. A. and Kew, W.: 4 - High-resolution mass spectrometry strategies for the investigation of dissolved  
573 organic matter, in: *Multidimensional Analytical Techniques in Environmental Research*, edited by: Duarte, R.  
574 M. B. O. and Duarte, A. C., Elsevier, 71–104, <https://doi.org/10.1016/B978-0-12-818896-5.00004-1>, 2020b.
- 575 Hawkes, J. A., Dittmar, T., Patriarca, C., Tranvik, L., and Bergquist, J.: Evaluation of the Orbitrap Mass  
576 Spectrometer for the Molecular Fingerprinting Analysis of Natural Dissolved Organic Matter, *Anal. Chem.*,  
577 88, 7698–7704, <https://doi.org/10.1021/acs.analchem.6b01624>, 2016.
- 578 Hawkes, J. A., D'Andrilli, J., Agar, J. N., Barrow, M. P., Berg, S. M., Catalán, N., Chen, H., Chu, R. K., Cole, R. B.,  
579 Dittmar, T., Gavard, R., Gleixner, G., Hatcher, P. G., He, C., Hess, N. J., Hutchins, R. H. S., Ijaz, A., Jones, H.  
580 E., Kew, W., Khaksari, M., Lozano, D. C. P., Lv, J., Mazzoleni, L. R., Noriega-Ortega, B. E., Osterholz, H.,  
581 Radoman, N., Remucal, C. K., Schmitt, N. D., Schum, S. K., Shi, Q., Simon, C., Singer, G., Sleighter, R. L.,  
582 Stubbins, A., Thomas, M. J., Tolic, N., Zhang, S., Zito, P., and Podgorski, D. C.: An international laboratory  
583 comparison of dissolved organic matter composition by high resolution mass spectrometry: Are we getting the  
584 same answer?, *Limnol. Oceanogr. Methods*, 18, 235–258, <https://doi.org/10.1002/lom3.10364>, 2020.
- 585 Hedges, J. I., Eglinton, G., Hatcher, P. G., Kirchman, D. L., Arnosti, C., Derenne, S., Evershed, R. P., Kögel-  
586 Knabner, I., de Leeuw, J. W., Littke, R., Michaelis, W., and Rullkötter, J.: The molecularly-uncharacterized  
587 component of nonliving organic matter in natural environments, *Org. Geochem.*, 31, 945–958,  
588 [https://doi.org/10.1016/S0146-6380\(00\)00096-6](https://doi.org/10.1016/S0146-6380(00)00096-6), 2000.
- 589 Hill, M. O.: Diversity and Evenness: A Unifying Notation and Its Consequences, *Ecology*, 54, 427–432,  
590 <https://doi.org/10.2307/1934352>, 1973.
- 591 Iknayan, K. J., Tingley, M. W., Furnas, B. J., and Beissinger, S. R.: Detecting diversity: emerging methods to  
592 estimate species diversity, *Trends Ecol. Evol.*, 29, 97–106, <https://doi.org/10.1016/j.tree.2013.10.012>, 2014.
- 593 Kaiser, N. K., McKenna, A. M., Savory, J. J., Hendrickson, C. L., and Marshall, A. G.: Tailored Ion Radius  
594 Distribution for Increased Dynamic Range in FT-ICR Mass Analysis of Complex Mixtures, *Anal. Chem.*, 85,  
595 265–272, <https://doi.org/10.1021/ac302678v>, 2013.
- 596 Kellerman, A. M., Dittmar, T., Kothawala, D. N., and Tranvik, L. J.: Chemodiversity of dissolved organic matter in  
597 lakes driven by climate and hydrology, *Nat. Commun.*, 5, 3804, <https://doi.org/10.1038/ncomms4804>, 2014.
- 598 Kim, D., Kim, S., Son, S., Jung, M.-J., and Kim, S.: Application of Online Liquid Chromatography 7 T FT-ICR  
599 Mass Spectrometer Equipped with Quadrupolar Detection for Analysis of Natural Organic Matter, *Anal.*





- 600 Chem., 91, 7690–7697, <https://doi.org/10.1021/acs.analchem.9b00689>, 2019.
- 601 Kruve, A., Kaupmees, K., Liigand, J., and Leito, I.: Negative Electrospray Ionization via Deprotonation: Predicting  
602 the Ionization Efficiency, *Anal. Chem.*, 86, 4822–4830, <https://doi.org/10.1021/ac404066v>, 2014.
- 603 Kujawinski, E. B., Longnecker, K., Blough, N. V., Vecchio, R. D., Finlay, L., Kitner, J. B., and Giovannoni, S. J.:  
604 Identification of possible source markers in marine dissolved organic matter using ultrahigh resolution mass  
605 spectrometry, *Geochim. Cosmochim. Acta*, 73, 4384–4399, <https://doi.org/10.1016/j.gca.2009.04.033>, 2009.
- 606 LaRowe, D. E. and Van Cappellen, P.: Degradation of natural organic matter: A thermodynamic analysis, *Geochim.  
607 Cosmochim. Acta*, 75, 2030–2042, <https://doi.org/10.1016/j.gca.2011.01.020>, 2011.
- 608 Leyva, D., Tose, L. V., Porter, J., Wolff, J., Jaffé, R., and Fernandez-Lima, F.: Understanding the structural  
609 complexity of dissolved organic matter: isomeric diversity, *Faraday Discuss.*, 218, 431–440,  
610 <https://doi.org/10.1039/C8FD00221E>, 2019.
- 611 Leyva, D., Jaffe, R., and Fernandez-Lima, F.: Structural Characterization of Dissolved Organic Matter at the  
612 Chemical Formula Level Using TIMS-FT-ICR MS/MS, *Anal. Chem.*, 92, 11960–11966,  
613 <https://doi.org/10.1021/acs.analchem.0c02347>, 2020.
- 614 Li, H.-Y., Wang, H., Wang, H.-T., Xin, P.-Y., Xu, X.-H., Ma, Y., Liu, W.-P., Teng, C.-Y., Jiang, C.-L., Lou, L.-P.,  
615 Arnold, W., Cralle, L., Zhu, Y.-G., Chu, J.-F., Gilbert, J. A., and Zhang, Z.-J.: The chemodiversity of paddy  
616 soil dissolved organic matter correlates with microbial community at continental scales, *Microbiome*, 6, 187,  
617 <https://doi.org/10.1186/s40168-018-0561-x>, 2018.
- 618 Li, Y., Harir, M., Uhl, J., Kanawati, B., Lucio, M., Smirnov, K. S., Koch, B. P., Schmitt-Kopplin, P., and Hertkorn,  
619 N.: How representative are dissolved organic matter (DOM) extracts? A comprehensive study of sorbent  
620 selectivity for DOM isolation, *Water Res.*, 116, 316–323, <https://doi.org/10.1016/j.watres.2017.03.038>, 2017.
- 621 Lucas, J., Koester, I., Wichels, A., Niggemann, J., Dittmar, T., Callies, U., Wiltshire, K. H., and Gerdt, G.: Short-  
622 Term Dynamics of North Sea Bacterioplankton-Dissolved Organic Matter Coherence on Molecular Level,  
623 *Front. Microbiol.*, 7, 2016.
- 624 Makarov, A., Denisov, E., Kholomeev, A., Balschun, W., Lange, O., Strupat, K., and Horning, S.: Performance  
625 Evaluation of a Hybrid Linear Ion Trap/Orbitrap Mass Spectrometer, *Anal. Chem.*, 78, 2113–2120,  
626 <https://doi.org/10.1021/ac0518811>, 2006.
- 627 Makarov, A., Grinfeld, D., and Ayzikov, K.: Chapter 2 - Fundamentals of Orbitrap analyzer, in: *Fundamentals and  
628 Applications of Fourier Transform Mass Spectrometry*, edited by: Kanawati, B. and Schmitt-Kopplin, P.,  
629 Elsevier, 37–61, <https://doi.org/10.1016/B978-0-12-814013-0.00002-8>, 2019.
- 630 Marshall, A. G., Hendrickson, C. L., and Jackson, G. S.: Fourier transform ion cyclotron resonance mass  
631 spectrometry: A primer, *Mass Spectrom. Rev.*, 17, 1–35, [https://doi.org/10.1002/\(SICI\)1098-  
2787\(1998\)17:1<1::AID-MAS1>3.0.CO;2-K](https://doi.org/10.1002/(SICI)1098-<br/>632 2787(1998)17:1<1::AID-MAS1>3.0.CO;2-K), 1998.
- 633 McGill, B. J., Etienne, R. S., Gray, J. S., Alonso, D., Anderson, M. J., Benecha, H. K., Dornelas, M., Enquist, B. J.,  
634 Green, J. L., He, F., Hurlbert, A. H., Magurran, A. E., Marquet, P. A., Maurer, B. A., Ostling, A., Soykan, C.  
635 U., Ugland, K. I., and White, E. P.: Species abundance distributions: moving beyond single prediction theories  
636 to integration within an ecological framework, *Ecol. Lett.*, 10, 995–1015, [https://doi.org/10.1111/j.1461-  
0248.2007.01094.x](https://doi.org/10.1111/j.1461-<br/>637 0248.2007.01094.x), 2007.
- 638 Merder, J., Röder, H., Dittmar, T., Feudel, U., Freund, J. A., Gerdt, G., Kraberg, A., and Niggemann, J.: Dissolved  
639 organic compounds with synchronous dynamics share chemical properties and origin, *Limnol. Oceanogr.*, n/a,  
640 <https://doi.org/10.1002/lno.11938>, 2021.
- 641 Mouillot, D. and Leprêtre, A.: A comparison of species diversity estimators, *Res. Popul. Ecol.*, 41, 203–215,  
642 <https://doi.org/10.1007/s101440050024>, 1999.
- 643 Osterholz, H., Singer, G., Wemheuer, B., Daniel, R., Simon, M., Niggemann, J., and Dittmar, T.: Deciphering  
644 associations between dissolved organic molecules and bacterial communities in a pelagic marine system,  
645 *ISME J.*, 10, 1717–1730, <https://doi.org/10.1038/ismej.2015.231>, 2016.
- 646 Patriarca, C. and Hawkes, J. A.: High Molecular Weight Spectral Interferences in Mass Spectra of Dissolved  
647 Organic Matter, *J. Am. Soc. Mass Spectrom.*, 32, 394–397, <https://doi.org/10.1021/jasms.0c00353>, 2021.
- 648 Raeke, J., Lechtenfeld, O. J., Wagner, M., Herzsprung, P., and Reemtsma, T.: Selectivity of solid phase extraction of

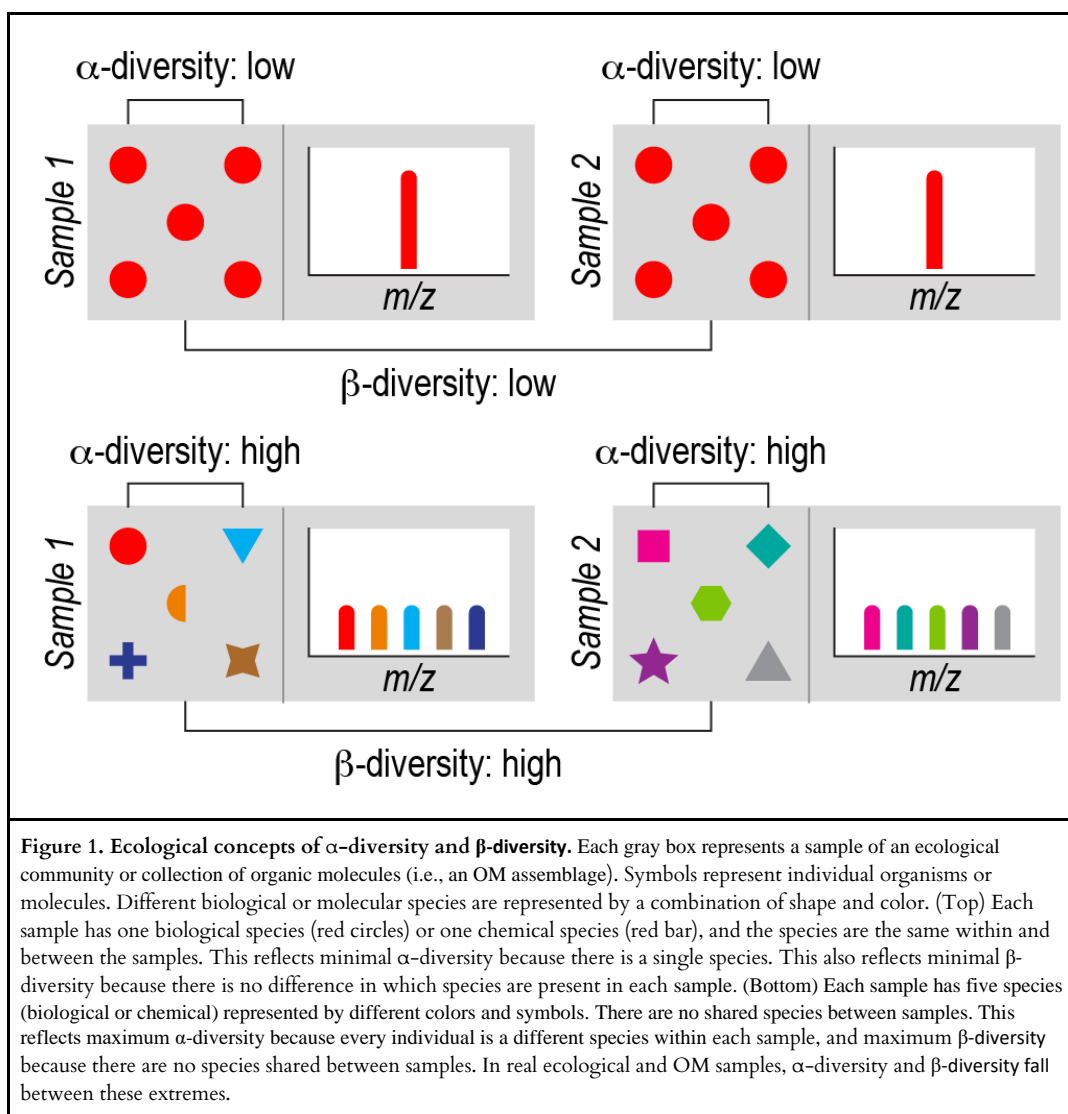




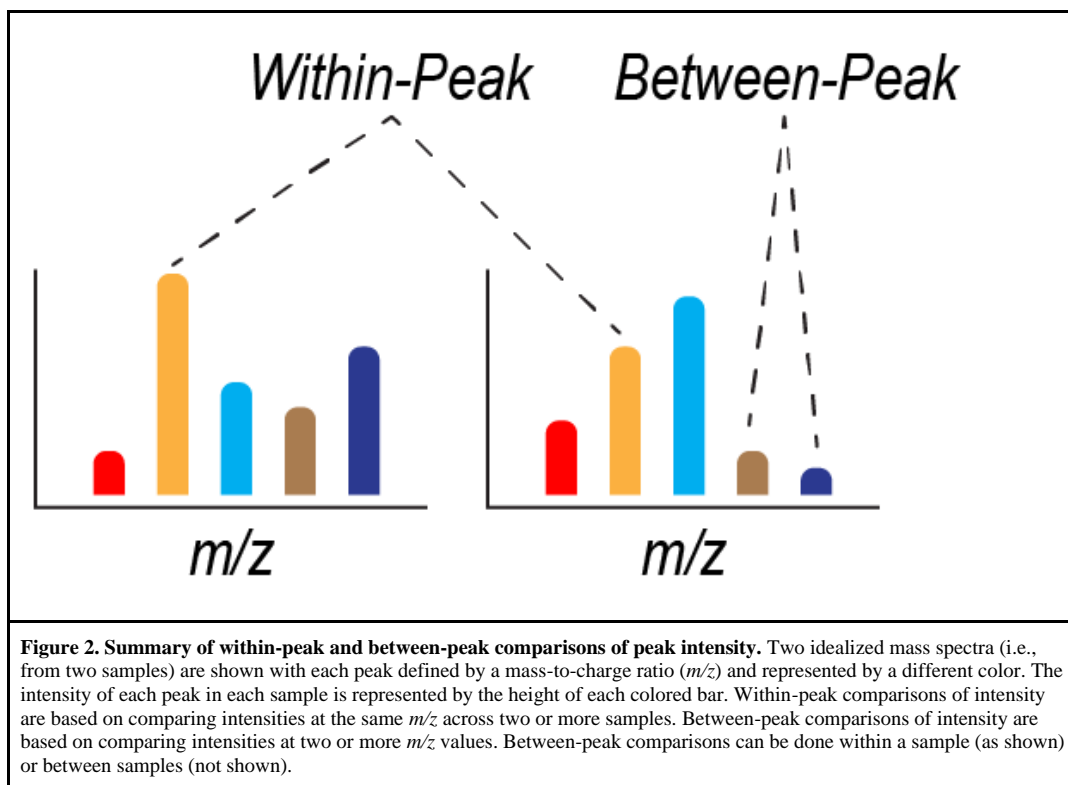
- 649 freshwater dissolved organic matter and its effect on ultrahigh resolution mass spectra, *Environ. Sci. Process.*  
650 *Impacts*, 18, 918–927, <https://doi.org/10.1039/C6EM00200E>, 2016.
- 651 Redowan, M.: Spatial pattern of tree diversity and evenness across forest types in Majella National Park, Italy, *For.*  
652 *Ecosyst.*, 2, 24, <https://doi.org/10.1186/s40663-015-0048-1>, 2015.
- 653 Richter, A., Nakamura, G., Agra Iserhard, C., and da Silva Duarte, L.: The hidden side of diversity: Effects of  
654 imperfect detection on multiple dimensions of biodiversity, *Ecol. Evol.*, 11, 12508–12519,  
655 <https://doi.org/10.1002/ece3.7995>, 2021.
- 656 Roth, T., Allan, E., Pearman, P. B., and Amrhein, V.: Functional ecology and imperfect detection of species,  
657 *Methods Ecol. Evol.*, 9, 917–928, <https://doi.org/10.1111/2041-210X.12950>, 2018.
- 658 Ruddy, B. M., Hendrickson, C. L., Rodgers, R. P., and Marshall, A. G.: Positive Ion Electrospray Ionization  
659 Suppression in Petroleum and Complex Mixtures, *Energy Fuels*, 32, 2901–2907,  
660 <https://doi.org/10.1021/acs.energyfuels.7b03204>, 2018.
- 661 Senko, M. W., Hendrickson, C. L., Emmett, M. R., Shi, S. D.-H., and Marshall, A. G.: External Accumulation of  
662 Ions for Enhanced Electrospray Ionization Fourier Transform Ion Cyclotron Resonance Mass Spectrometry, *J.*  
663 *Am. Soc. Mass Spectrom.*, 8, 970–976, [https://doi.org/10.1016/S1044-0305\(97\)00126-8](https://doi.org/10.1016/S1044-0305(97)00126-8), 1997.
- 664 Shaw, J. B., Lin, T.-Y., Leach, F. E., Tolmachev, A. V., Tolić, N., Robinson, E. W., Koppelaar, D. W., and Paša-  
665 Tolić, L.: 21 Tesla Fourier Transform Ion Cyclotron Resonance Mass Spectrometer Greatly Expands Mass  
666 Spectrometry Toolbox, *J. Am. Soc. Mass Spectrom.*, 27, 1929–1936, <https://doi.org/10.1007/s13361-016-1507-9>, 2016.
- 668 Smith, D. F., Podgorski, D. C., Rodgers, R. P., Blakney, G. T., and Hendrickson, C. L.: 21 Tesla FT-ICR Mass  
669 Spectrometer for Ultrahigh-Resolution Analysis of Complex Organic Mixtures, *Anal. Chem.*, 90, 2041–2047,  
670 <https://doi.org/10.1021/acs.analchem.7b04159>, 2018.
- 671 Steen, A. D., Kusch, S., Abdulla, H. A., Cakić, N., Coffinet, S., Dittmar, T., Fulton, J. M., Galy, V., Hinrichs, K.-U.,  
672 Ingalls, A. E., Koch, B. P., Kujawinski, E., Liu, Z., Osterholz, H., Rush, D., Seidel, M., Sepúlveda, J., and  
673 Wakeham, S. G.: Analytical and Computational Advances, Opportunities, and Challenges in Marine Organic  
674 Biogeochemistry in an Era of “Omics,” *Front. Mar. Sci.*, 7, 2020.
- 675 Tanentzap, A. J., Fitch, A., Orland, C., Emilson, E. J. S., Yakimovich, K. M., Osterholz, H., and Dittmar, T.:  
676 Chemical and microbial diversity covary in fresh water to influence ecosystem functioning, *Proc. Natl. Acad.*  
677 *Sci.*, 116, 24689–24695, <https://doi.org/10.1073/pnas.1904896116>, 2019.
- 678 Tose, L. V., Benigni, P., Leyva, D., Sundberg, A., Ramírez, C. E., Ridgeway, M. E., Park, M. A., Romão, W., Jaffé,  
679 R., and Fernandez-Lima, F.: Coupling trapped ion mobility spectrometry to mass spectrometry: trapped ion  
680 mobility spectrometry–time-of-flight mass spectrometry versus trapped ion mobility spectrometry–Fourier  
681 transform ion cyclotron resonance mass spectrometry, *Rapid Commun. Mass Spectrom.*, 32, 1287–1295,  
682 <https://doi.org/10.1002/rcm.8165>, 2018.
- 683 Whittaker, R. H.: Evolution and Measurement of Species Diversity, *TAXON*, 21, 213–251,  
684 <https://doi.org/10.2307/1218190>, 1972.
- 685 Wörner, T. P., Snijder, J., Bennett, A., Agbandje-McKenna, M., Makarov, A. A., and Heck, A. J. R.: Resolving  
686 heterogeneous macromolecular assemblies by Orbitrap-based single-particle charge detection mass  
687 spectrometry, *Nat. Methods*, 17, 395–398, <https://doi.org/10.1038/s41592-020-0770-7>, 2020.
- 688 Zark, M., Christoffers, J., and Dittmar, T.: Molecular properties of deep-sea dissolved organic matter are predictable  
689 by the central limit theorem: Evidence from tandem FT-ICR-MS, *Mar. Chem.*, 191, 9–15,  
690 <https://doi.org/10.1016/j.marchem.2017.02.005>, 2017.
- 691  
692



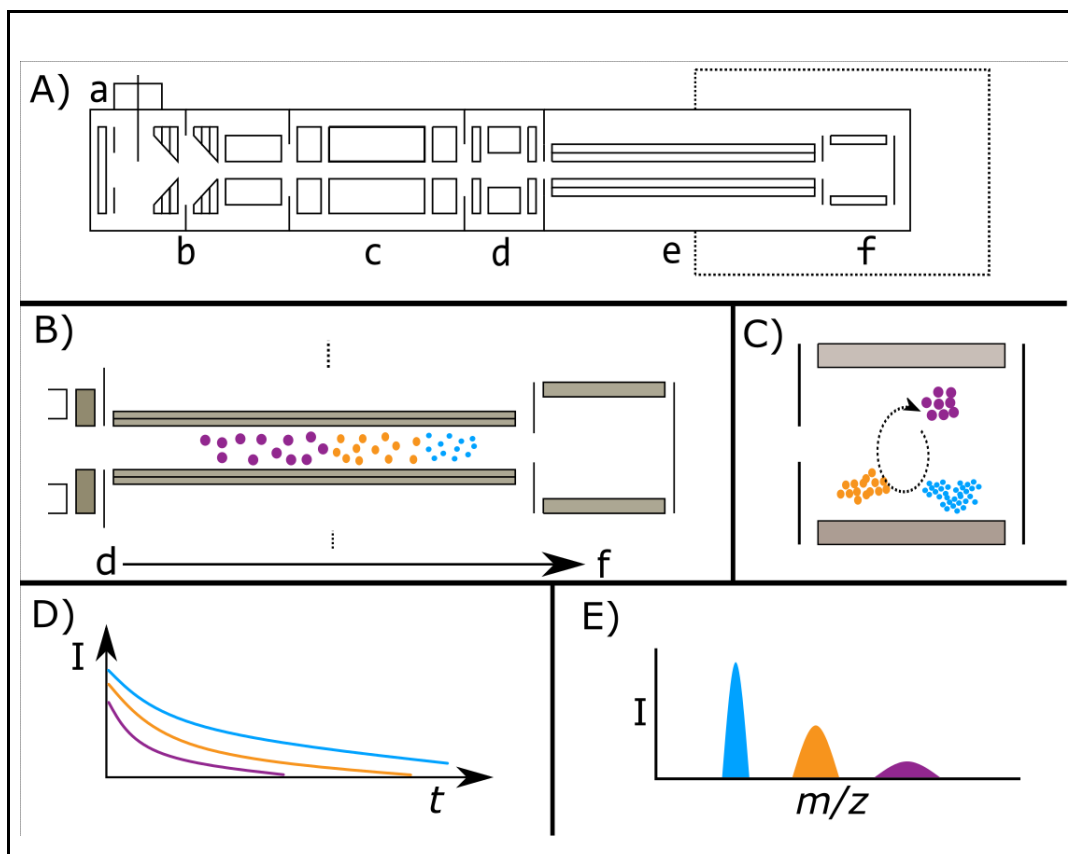
693 **Figures**  
694



695  
696

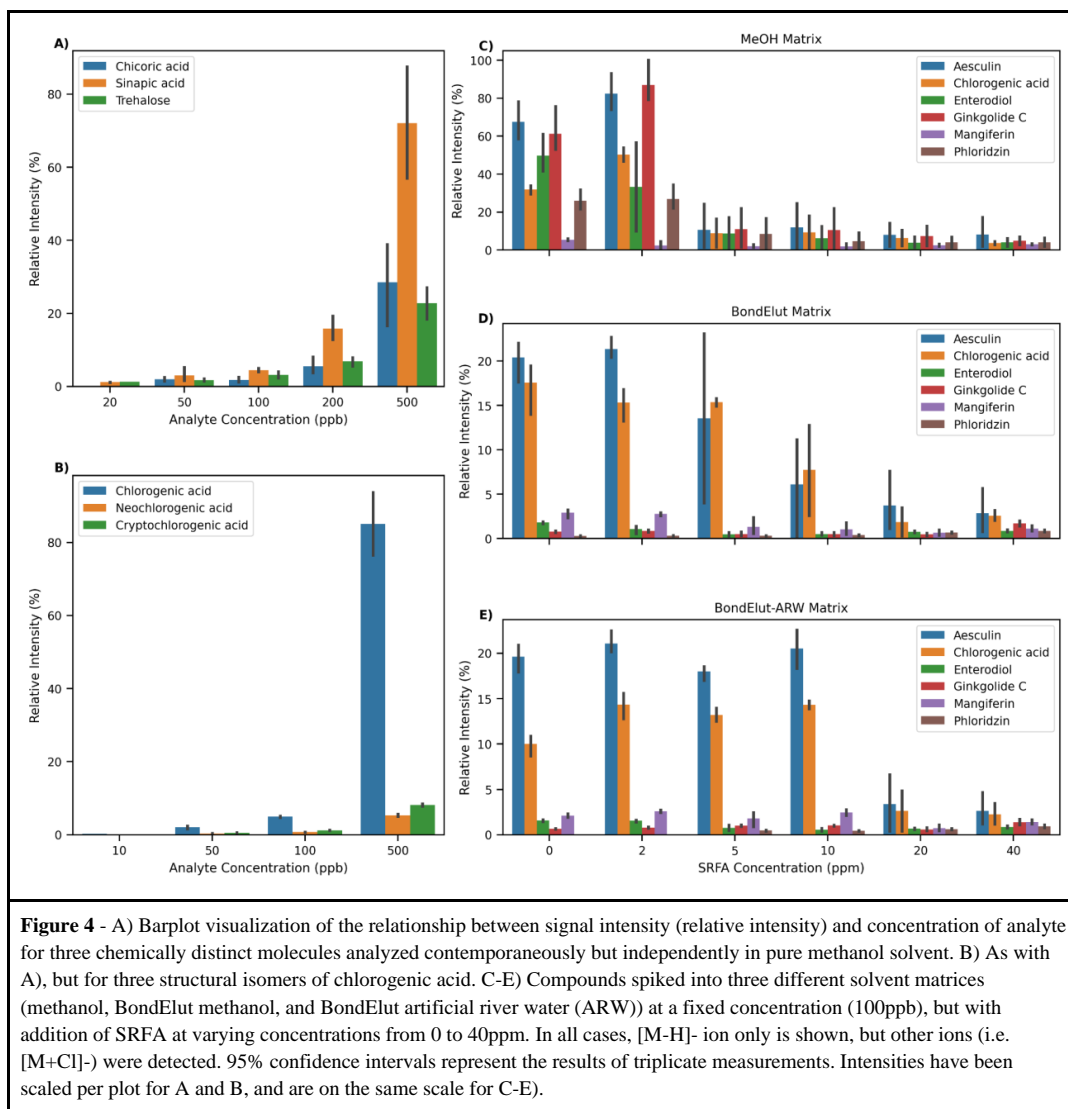


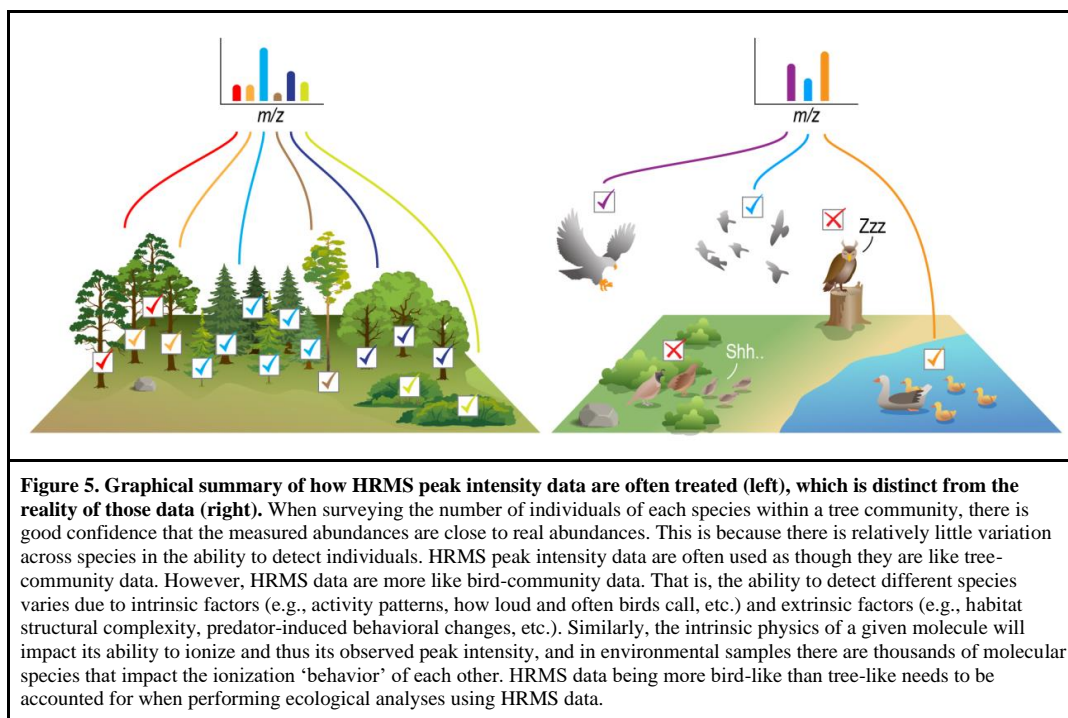
697



**Figure 3. Illustrative example of a generic FTICR mass spectrometer (panel A), showing common and key biases between FTICR signal intensity and  $m/z$  of ions (B-E).** Panel A shows the major elements of a generic FTICR mass spectrometer (based loosely on a Bruker solariX FTICR MS geometry). Panel A elements include; a - atmospheric pressure ionization source (i.e. ESI source), b - source ion optics (i.e. dual ion funnels), c - mass selecting quadrupole, d - collision cell, e - transfer multipoles to ICR cell, f - ICR cell. Dashed line indicates the magnetic field. Note: diagram is deliberately simplified and not to scale. Panel B) demonstrates the time-of-flight bias along the transfer multipoles (e) in the ‘flight tube’, from the collision cell (d) to the ICR cell (f). Lower  $m/z$  ions travel faster, as indicated by the smaller icons reaching the ICR cell first. Ions are shaded to aid visualization. Panel C) visualizes the effect of a variable excitation radii for ions of different masses, as may happen with a CHIRP excitation pulse. Lower  $m/z$  ions are closer to the detection electrodes (shaded in gray) and therefore will induce a larger image current. Note also the ion populations have been adjusted from B) to indicate biases from the time-of-flight effect. Panel D) shows the time-domain recorded signal intensity against time, with the ions having an initial intensity roughly proportional to the number of ions in that cloud. However, as time progresses the less abundant ion clouds lose coherence and destabilize more rapidly, resulting in an attenuation of their signal. Note that the real signal would follow a damped sinusoidal function; here an absolute value approximation is shown for simplicity. Panel E) shows the mass spectrum post-Fourier transform, demonstrating that the impact is not only on intensity (peak height), but also resolution (peak width). In all cases, effects are deliberately exaggerated and not-to-scale to aid interpretation.

698  
699





701





702

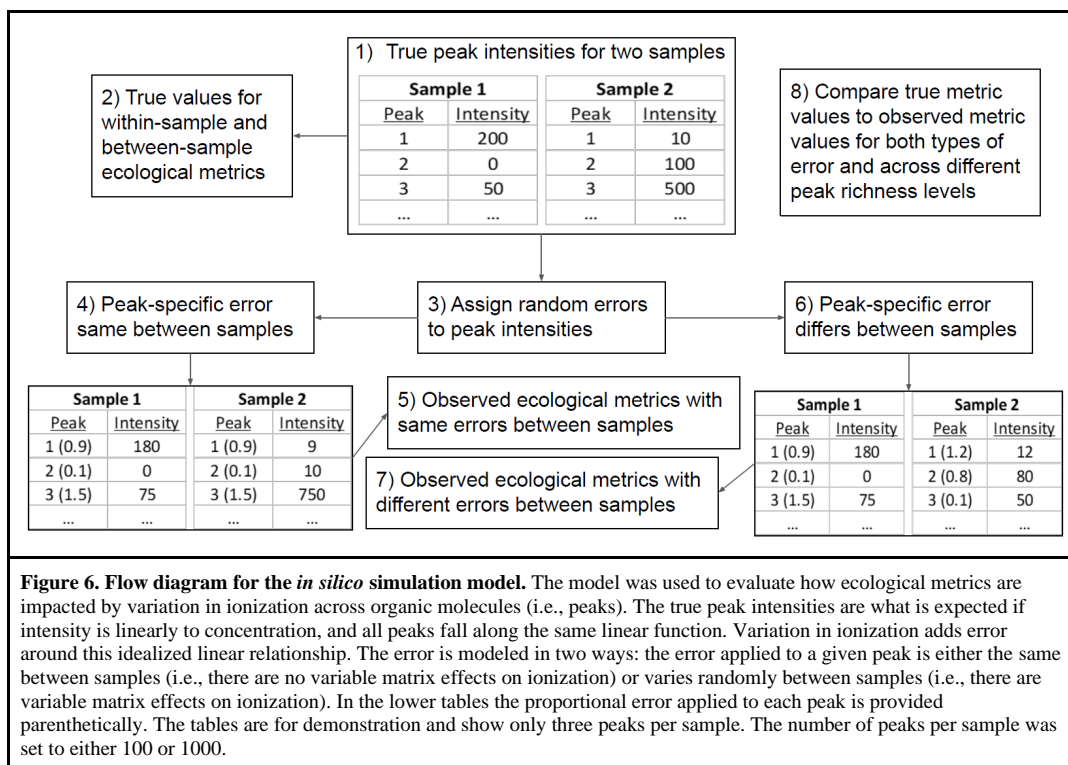
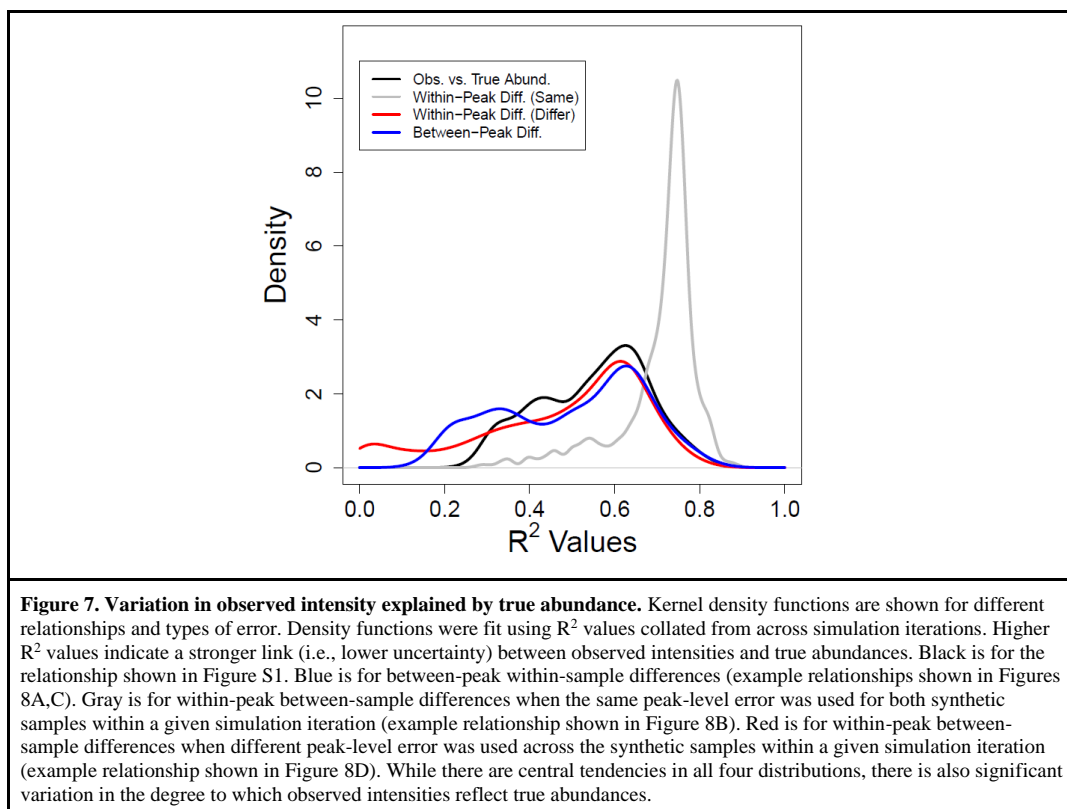


**Figure 6. Flow diagram for the *in silico* simulation model.** The model was used to evaluate how ecological metrics are impacted by variation in ionization across organic molecules (i.e., peaks). The true peak intensities are what is expected if intensity is linearly to concentration, and all peaks fall along the same linear function. Variation in ionization adds error around this idealized linear relationship. The error is modeled in two ways: the error applied to a given peak is either the same between samples (i.e., there are no variable matrix effects on ionization) or varies randomly between samples (i.e., there are variable matrix effects on ionization). In the lower tables the proportional error applied to each peak is provided parenthetically. The tables are for demonstration and show only three peaks per sample. The number of peaks per sample was set to either 100 or 1000.

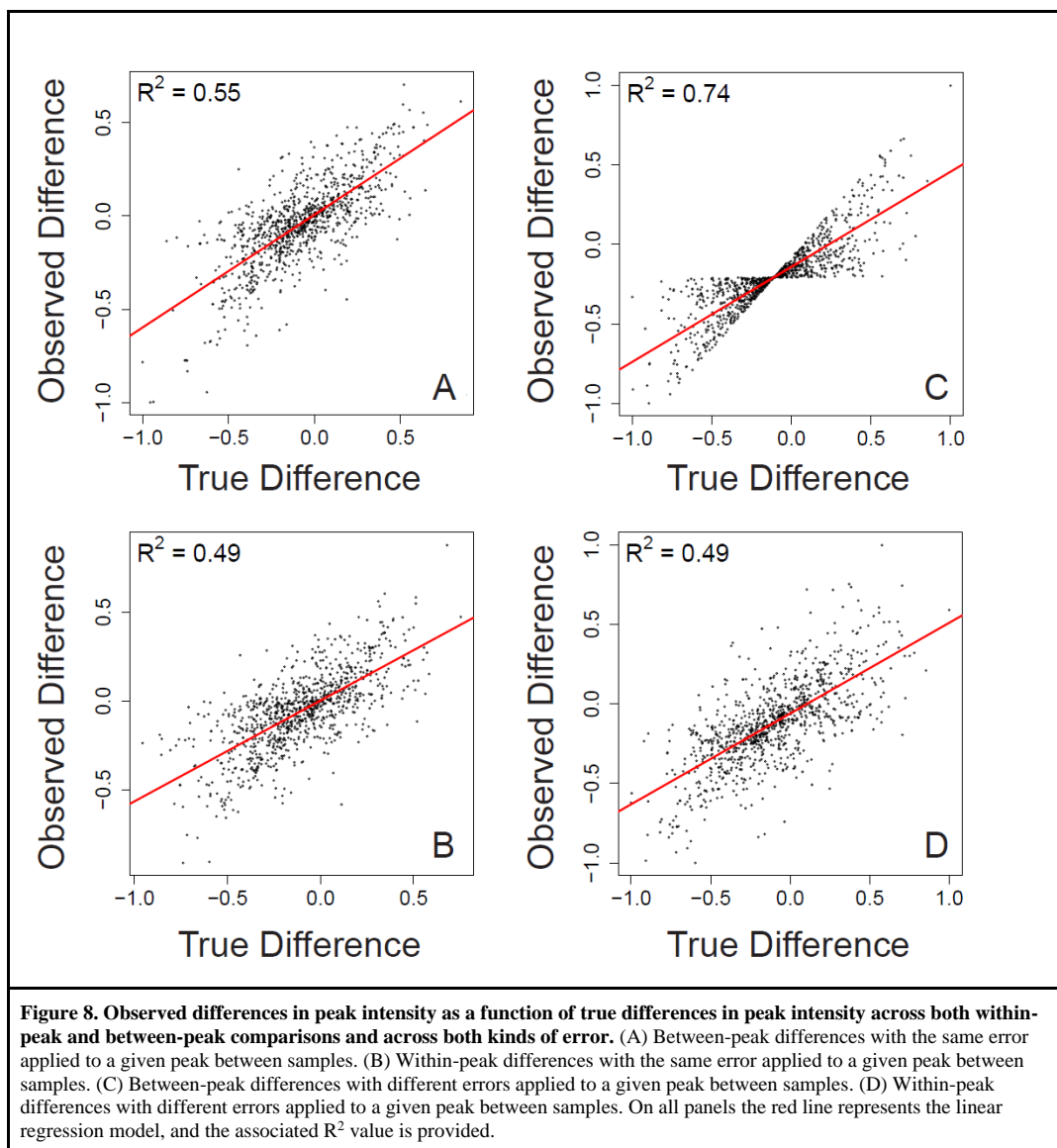
703



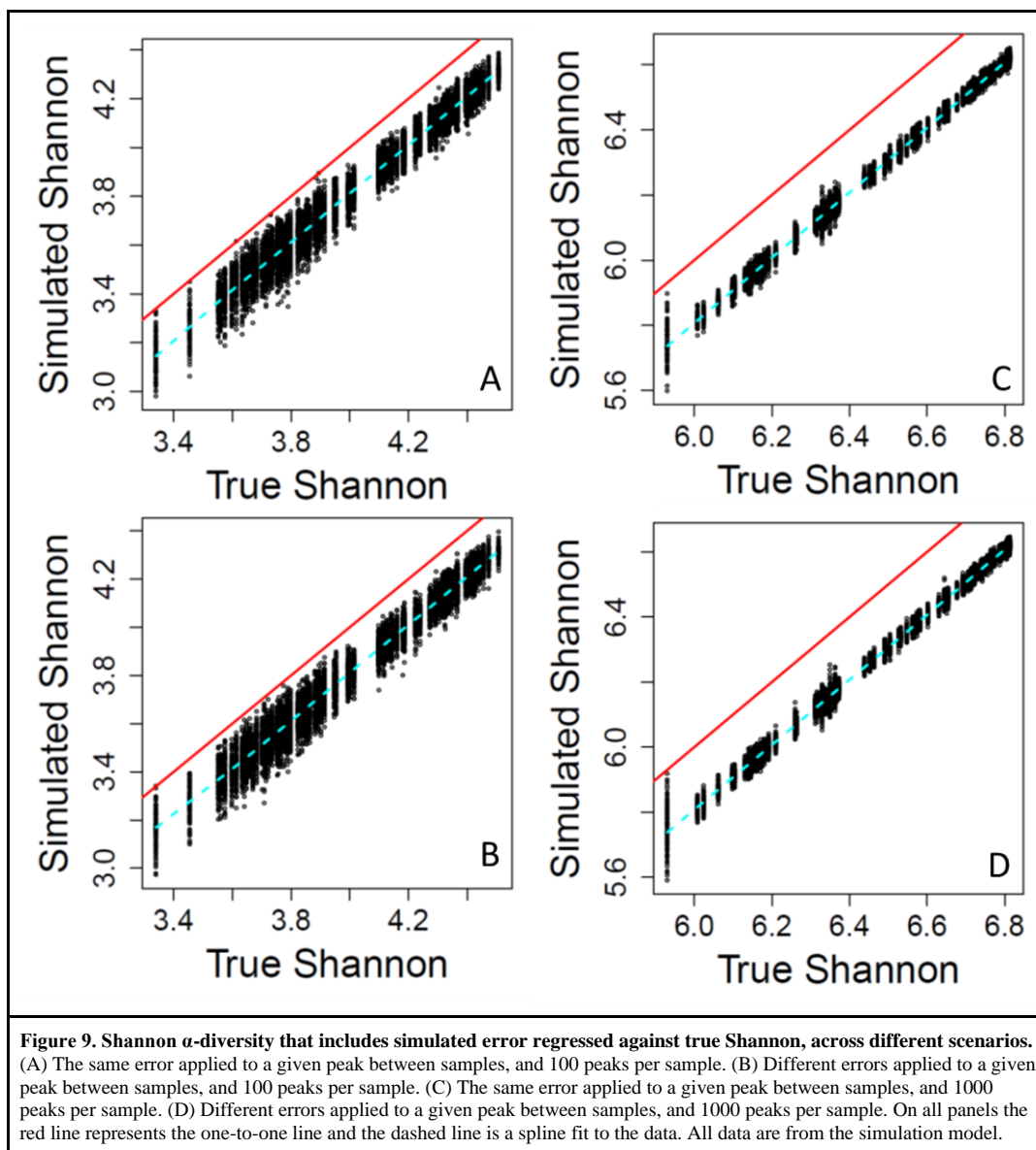
704



705



706



707

